 doi:10.20944/preprints202107.0539.v1

Article

Evaluation of the uniformity of protective coatings on concrete structure surfaces based on cluster analysis

Dunwen Liu [1], Wanmao Zhang [1], Yu Tang [1,*], Yinghua Jian [1], Chun Gong [1] and Fengkai Qiu [1]

[1] School of Resources and Safety Engineering, Central South University, Changsha 410083, China; dunwen@csu.edu.cn (D.L.); 205512136@csu.edu.cn (W.Z.); jyh__0412@csu.edu.cn (Y.J.); gongchun@csu.edu.cn (C.G.); 1772156946@qq.com (F.Q.)

* Correspondence: tangyu9433@163.com

Abstract: With the continuous development of urbanization and industrialization in the world, concrete is widely used in various engineering constructions as an engineering material. However, the consequent problem of durability of concrete structures is also becoming increasingly prominent. As an important additional measures, protective coating can effectively improve the durability of concrete performance. Moreover, the uniformity of the concrete surface coating will directly affect its protective effect. Therefore, we propose a nondestructive inspection and evaluation method of coating uniformity based on infrared imaging and cluster analysis for concrete surface coating uniformity detection and evaluation. Based on the obtained infrared images, a series of processing and analysis of the images were carried out using MATLAB software to obtain the characteristics of the infrared images of concrete surface. Finally, by extracting the temperature distribution data of the pixel points on the concrete surface, an evaluation method of concrete surface coating uniformity based on a combination of cluster analysis and hierarchical analysis was established. The evaluation results show that the determination results obtained by this method are consistent with the actual situation. This study has a positive contribution to the testing of concrete surface coating uniformity and its evaluation.

Keywords: concrete protection; infrared detection; image processing; cluster analysis; uniformity evaluation

1. Introduction

Concrete structures are subjected to chloride ion attack, sulfate corrosion, and carbonation corrosion during service. These accelerate the deterioration of material properties, and can lead to structural failure or even destruction in severe cases 1. In the early 20th century, statistical studies on concrete corrosion found that the cost of repair and reinforcement of structures due to concrete corrosion was several times higher than the cost of new construction. The results of corrosion cost surveys in China found that corrosion costs in 2014 were as high as RMB 2.1 trillion, accounting for 3.34% of the GDP in that year 2. Therefore, the corrosion of concrete structures not only involves structural safety, but also involves ecological civilization issues, energy conservation issues and economic issues. It is necessary to carry out research on corrosion prevention of concrete.

Experts from different countries have carried out a lot of research for concrete corrosion protection. Concrete material ratios and microstructures have been optimized. These not only enhance the strength of concrete, but also improve the anti-corrosion performance 3. However, with the development of civil engineering structures towards deep sea and mountainous areas, coupled with the frequent occurrence of global climate extremes, the structure environment has become more complex. The structure is not only subject to dynamic and static loading, and the corrosion of the structure by environmental

and biological factors cannot be ignored. Therefore, in order to improve the corrosion resistance and durability of concrete structures, protection of the surface of critical parts of concrete structures is proposed 4. Under the premise of not changing the property of concrete material, the protective coating can increase the functional characteristics of concrete. And it is widely used in engineering construction. Liliana Baltazar 5, Sang-SoonPark 6 and others have conducted extensive studies on the enhancement effect of inorganic silicate type coatings such as sodium silicate on concrete surfaces. In contrast to inorganic silicate coatings, research on organic and hybrid coatings has focused more on the development and preparation of new coatings. T.S. Velayutham 7, Aruz Petcherdchoo 8, and Paola Scarfato 9 prepared polyurethane (PUR) coatings, organosilane coatings, and polymer clay nanocomposite coatings. composite coatings, etc.

However, the construction process of spraying protective coatings on the surface of concrete structures is prone to defects such as uneven thickness, porosity, and inclusions 10. These defects can affect the protective performance of the coating to varying degrees and even lead to coating protection failure. Especially when the anticorrosive silane spraying on the surface of the concrete pipe sheet in the tunnel is not uniform. The aggressive ions contained in the water body can easily pass through the weak part of the silane spraying on the surface of the pipe sheet, and cause local corrosion to the pipe sheet. Therefore, the uniformity test of silane spraying on tunnel pipe sheet is extremely important for its corrosion resistance and durability during operation.

At present, there are few studies on the uniformity testing of spraying protective coatings on concrete surfaces. In the actual engineering application, it mainly relies on the visual inspection method. The method is mostly subjective judgment by the naked eye of the inspector, which lacks scientific basis and its accuracy is difficult to be guaranteed. In recent years, with the improvement of the accuracy of infrared imaging systems and the rapid development of image processing technology, infrared thermal imaging technology has gradually made significant breakthroughs in modern industry, medical and biological fields 11. Infrared imaging as a nondestructive testing and analysis tool has demonstrated powerful advantages. The study of its detection mechanism and application fields has received a lot of attention from scholars. From the current stage of research on infrared imaging detection technology. The research content mainly focuses on the design of infrared imager system, applied excitation method and infrared image processing and applicability 14. Therefore, infrared thermal imaging technology has a broad application prospect in the analysis of uniformity detection of protective coatings on concrete surfaces.

In general, the temperature resolution and contrast of the images obtained from thermal imaging cameras are generally low due to the limitations of their own performance. Moreover, the images also contain various noises, which bring a very negative impact on the detection and analysis of the target. Based on these problems, many researchers at home and abroad have conducted in-depth studies on the correction of detector inhomogeneities, and the removal of periodic noise, etc 19. The research results have an important role in promoting the development of infrared image processing technology. However, there are still certain errors in the processed infrared images. In order to realize the use of infrared imaging technology to detect the uniformity of concrete surface coating, it is necessary to carry out a series of processing of infrared images. In this paper, based on the MATLAB software function tool, the infrared thermal images obtained from the experiments are processed in a relevant way. Finally, the uniformity of the coating is determined qualitatively by the distribution of the surface areas of the images.

In the process of infrared imaging inspection experiments, the thermal imaging camera collects the surface temperature distribution of each concrete specimen at different frames. For the massive amount of data, it is impossible to continue the analysis by the traditional manual analysis means. With the rapid development of modern computer operation speed and the in-depth research on data processing methods, it is possible to use artificial intelligence method to confirm the results of experimental data prediction with those obtained from engineering experiments 21. Clustering analysis is an unattended

learning method in machine learning in the field of artificial intelligence. In addition to machine learning, it can be used for statistics, spatial data mining and image recognition. In this statistical algorithm, grouping programs such as S-Plus, SPSS and SAS are used intensively, which utilize K-means and cluster analysis methods 22. There are two types of clustering in MATLAB, including hierarchical clustering and K-means clustering 23. K-means clustering was invented by MacQueen in 1967 25 and it is one of the most commonly used unattended learning methods. K-means clustering possesses an assignment mechanism that allows each dataset to belong to only one cluster, so that each point in the dataset is assigned to its nearest node clustering 26. The ease of implementation and fast operation on large datasets are the main advantages of K-means clustering.

Therefore, this study addresses the current problems of homogeneity testing of silane coatings. Infrared imaging nondestructive testing technology is used, combined with cluster analysis to statistically analyze the infrared imaging data, so as to achieve the evaluation of the homogeneity of silane coatings. The main research objectives include: (1) carry out experimental research on infrared imaging inspection of concrete surface coatings and obtain the temperature distribution images of concrete coating structure surfaces; (2) perform a series of processing of the acquired infrared images based on MATLAB software and qualitatively determine the homogeneity of the concrete surface coating using morphological processing methods; (3) according to the large sample data of temperature distribution of each pixel point on the concrete surface at different moments, a new method based on a combination of cluster analysis and hierarchical analysis is proposed for determining the uniformity of concrete surface coating.

2. Materials and Methods

2.1. Infrared Imaging Detection of Silane Coatings

2.1.1. Infrared Imaging Test Principle

Infrared imaging system is essentially a device that converts different electrical signals based on the temperature and emissivity of the natural scene. It generates a displayable infrared image by mapping the received infrared radiation energy of a target into grayscale values through an infrared detector. When the intensity of the infrared radiation of the target is higher, its grayscale value reflected in the infrared image is larger 28. The infrared imaging system mainly consists of an electrical signal processing system, an image processing system, an optical system, and an infrared detector. The working principle of the IR imaging system is as follows.

(1) Infrared radiation from the target, background and various interferences is transmitted in the atmosphere and reaches the infrared optical system after a certain attenuation effect.

(2) The optical system focuses the infrared radiation and then transmits the radiation to the infrared detector.

(3) Infrared detectors convert the received infrared radiation into current signals of different strengths and weaknesses.

(4) Transmission of the output electrical signal to an electrical signal processing system and enhancement by an amplifier therein.

(5) The amplified electrical signal is transformed into a two-dimensional graphic that can be viewed directly on a computer after passing through an image processing system.

2.1.2. Infrared Imaging Test Program

The main component of this test silane coating is 2,4,4-trimethylpentyltriethoxysilane with molecular formula C14H32O3Si. Silane is colorless liquid at room temperature, boiling point 236℃, density 0.88g/cm^3. The test used infrared bulb as thermal excitation source to apply continuous heat flow excitation to concrete structure. And an infrared imaging system was constructed with a SC7000 infrared camera from FLIR.

 doi:10.20944/preprints202107.0539.v1

The test blocks were obtained from the cores of the subway tunnel tube pieces and made into cylinders of 5cm in diameter and 10cm in height. Three groups of tests were designed according to the different degree of uniformity of the sprayed silane. They were classified as more uniform (N1), non-uniform (N2) and very non-uniform (N3). The infrared detection test system is shown in Figure 1, and the flow chart of this study is shown in Figure 2.

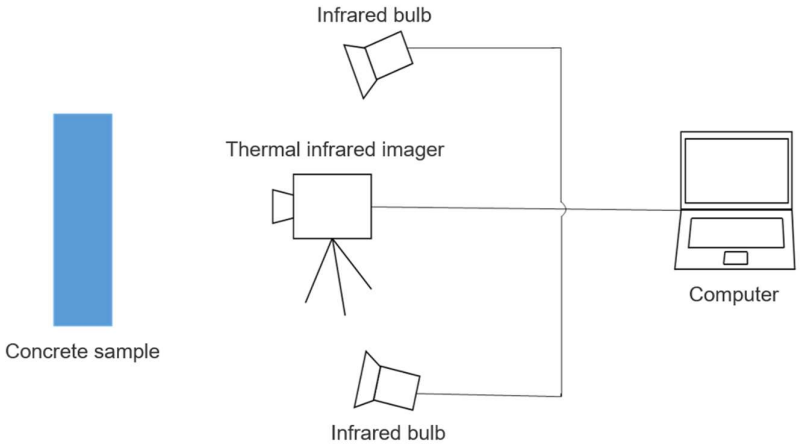

Figure 1. Infrared imaging detection system.

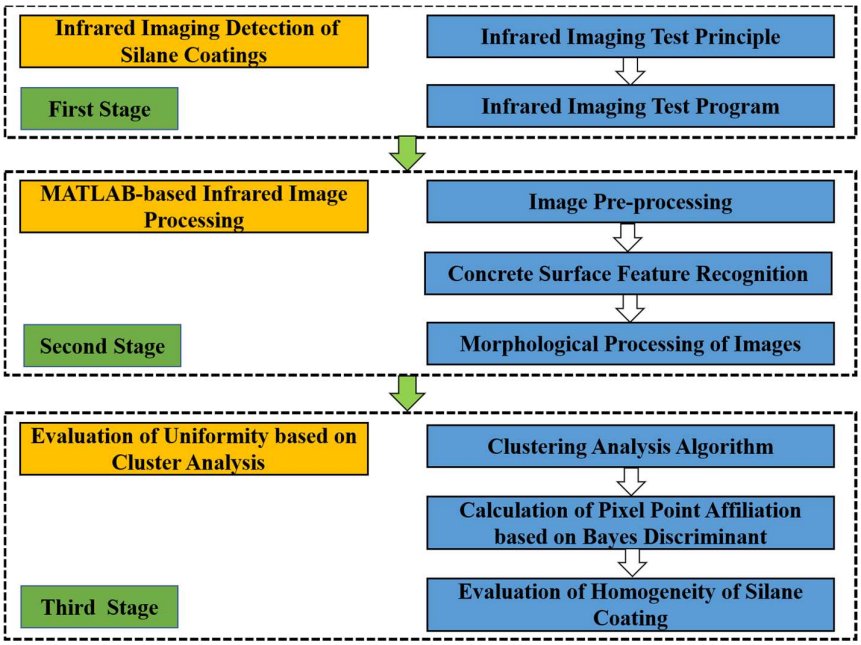

Figure 2. Flow chart of this study.

2.2. MATLAB-based Infrared Image Processing

Infrared images characterize the infrared radiation distribution of an object. The overall grayscale distribution of the image is low, and the image is prone to grayscale concentration. In addition, during the actual imaging process, noise sources from the external environment may lead to multiple noise in the infrared image, which affects the information of the infrared image itself. Therefore, a series of image processing is needed for IR images.

 doi:10.20944/preprints202107.0539.v1

2.2.1. Image Pre-Processing

Before image analysis, pre-processing operations need to be performed according to its features to enhance the contrast of the image. It facilitates the extraction of image features in the subsequent processing and improves the accuracy of the determination results. The pre-processing process generally includes image quality evaluation, image noise removal, image sharpening, etc 29.

1. Image quality evaluation

Commonly used objective evaluation metrics include entropy, standard deviation, etc. Among them, entropy reflects the information contained in the image. The higher the entropy is, the more information the image contains. The standard deviation represents the dispersion of the grayscale of an image relative to the average grayscale of the image. The larger the standard deviation, the more hierarchical the image is. Based on the entropy and std2 function in MATLAB, the evaluation index values of the three frames with better subjective evaluation quality in the infrared images in the experimental group A are derived respectively. And select the best infrared image quality for image analysis.

2. Image noise removal

The noise of image signal can be regarded as interference signal, which has random nature. Statistical features are commonly used to describe the noise, such as distribution functions and probability density functions of mean, variance, correlation functions, etc. In this study, median filtering method is used to remove it. The median filtering operation is implemented based on the medfilt2 function in MATLAB.

3. Image sharpening

In order to extract the features of concrete surface area, enhance the contour shape of the image and make the edge information of concrete image more prominent, the image sharpening method is used for the corresponding processing. The gradient method is often used in MATLAB to achieve image sharpening. For an image f (x, y), the gradient at (x, y) is defined as

$$grad(x,y)=(f'_x,f'_y)=\left(\frac{\partial f(x,y)}{\partial x},\frac{\partial f(x,y)}{\partial y}\right), \quad (1)$$

Where the gradient is a vector quantity with direction and magnitude. There are several different computational operators depending on how the gradient size is calculated. The common ones are mainly Laplacian operator, Prewitt operator, Sobel operator, etc. Among them, the Sobel operator adds the factor of weighted average to make the pixels on both sides of the edges in the image smooth. The obtained pre-processing images are shown in Figure 3.

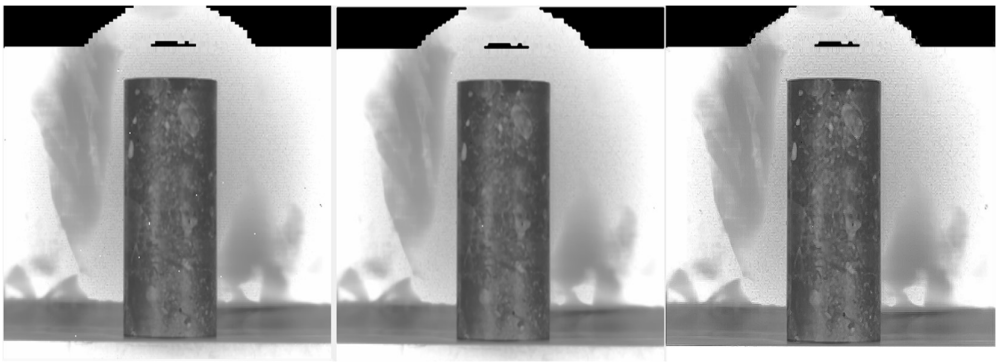

(**a**) (**b**) (**c**)

Figure 3. Concrete IR image pre-processing results: (a) image quality evaluation; (b) image noise removal; (c) image sharpening.

 doi:10.20944/preprints202107.0539.v1

By pre-processing the infrared image, the concrete image edge information is clearer and the surface area detail features are more obvious. A good foundation was laid for the subsequent edge detection processing.

2.2.2. Concrete Surface Feature Recognition

1. Image edge detection

In image processing, the region of interest in an image is generally referred to as the target (ROI), while the rest of the image is referred to as the background. Based on this principle, edge detection and segmentation of image targets can be achieved. In infrared images, the grayscale value of pixels at the target edge changes significantly, creating a discontinuity. For edges with step changes, the first-order derivative can be used to detect whether a point in the image is an edge point. The second-order derivative can be used to determine whether a pixel point lies to the left or right of an edge.

In image processing, edge detection can be accomplished by convolution with differential operators 32. Differential operators are divided into first-order differential operators and second-order operators. Commonly used first-order operators include Roberts operator, Prewitt operator and Sobel operator. Commonly used second-order operators include Log operator, Laplacian operator and so on. In this study, the second-order Log operator was used for edge detection processing.

2. Image segmentation and binarization based on thresholding

At present, a large number of analytical and computational methods have been formed for image segmentation, such as segmentation techniques by setting thresholds, segmentation based on genetic algorithms, etc. Among them, the image segmentation based on the threshold method has the advantages of large applicability, high operational efficiency and speed. The calculation formula of threshold method is:

$$g(i,j)=\begin{cases}1 & f(i,j)\geq T\\ 0 & f(i,j)\leq T'\end{cases} \tag{2}$$

where g (i, j) denotes the pixel value of the input image; f (i, j) denotes the pixel value of the output image; and T represents the threshold.

When for the target pixel of the image g (i, j) = 0, the background pixel of the image g (i, j) = 1. When the threshold value is determined, the grayscale value of each pixel point in the image is compared with the threshold value. In turn, two different regions of the image segmentation can be obtained.

An iterative algorithm is used for the calculation of the threshold values. The maximum gray value and the minimum gray value of the image were obtained based on the gray statistics of the concrete infrared image. And the threshold value T=0.5373 was obtained. After determining the threshold size, the image segmented by iterative thresholding method was obtained based on MATLAB.

2.2.3. Morphological Processing of Images

There are incomplete edges and voids in regions present in the threshold-segmented infrared images of concrete. The binary image is processed by morphological method. The processing operation of binary images can be realized by using the mathematical morphology method. Based on the closed operation in image morphology processing, MATLAB is applied to connect the broken edges and fill the holes, etc 34. The morphologically processed concrete image is obtained, as shown in Figure 4.

Preprints (www.preprints.org) | NOT PEER-REVIEWED | Posted: 23 July 2021 doi:10.20944/preprints202107.0539.v1

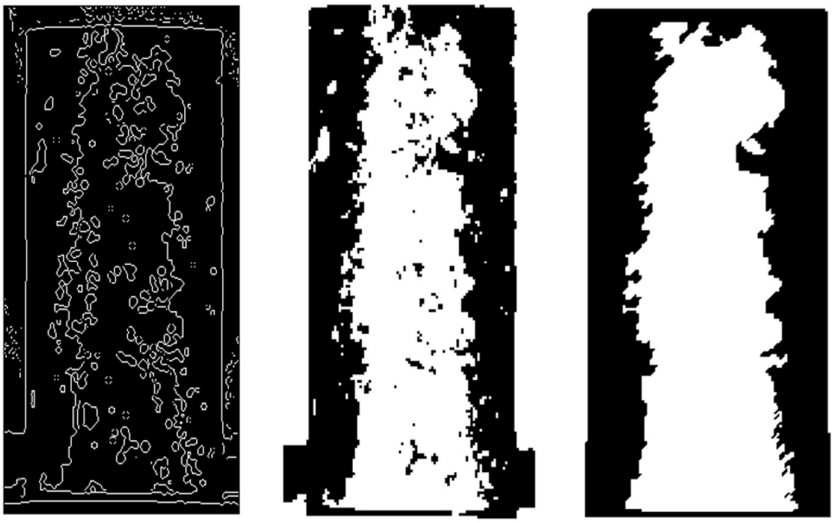

(**a**) (**b**) (**c**)

Figure 4. Concrete infrared image processing results: (a) edge detection processing; (b) binarization processing; (c) morphology processing.

2.3. Evaluation of Uniformity based on Cluster Analysis

2.3.1. Clustering Analysis Algorithm

Combining the principles of algorithm selection and the characteristics of each algorithm, this study adopts the k-means algorithm for clustering analysis of pixel point temperature data. k-means algorithm firstly selects k initial centroids randomly as clustering centers in a determined object containing n samples. The Euclidean distance is used to calculate the distance between other samples and the cluster center, and the sample points are grouped into the class with the closest distance to the cluster center. Then the mean value of each class is used as the new clustering center, and the samples are re-classified into k classes 35. And so on, iterative calculations are performed until the cluster centroids no longer change. k value is the number of classes, and the sum of the squared errors (SSE) is used to determine.

$$SSE = \sum_{i=1}^{k} \sum_{p \subseteq C_i} |p - m_i|^2 , \tag{3}$$

where C_i denotes the i-th cluster, p is any sample point in C_i, and m_i denotes the mean point of all samples in C_i. SSE is the sum of squared clustering errors for all samples. The degree of merit of the cluster analysis results can be measured, and thus the appropriate k value can be determined.

2.3.2. Calculation of Pixel Point Affiliation based on Bayes Discriminant

In order to determine the loss of misclassified concrete surface pixel points, the posterior probability that a pixel point belongs to some overall, i.e., the affiliation degree, is obtained. The Bayes discriminant method is used for discriminant analysis of the classification of each pixel point on the concrete surface 37. The basic idea is to assume the prior probability distribution of a known object. Then the hypothesis is corrected by some actual sample of the known object. Finally, the posterior probability distribution is obtained.

Suppose k p-dimensional overall $G_1, G_2, \cdots, G_k$, with density function $f_j(x)$, and prior probability $p_j = P(G_j)$, j=1, 2, 3, ..., *k*. Note that the posterior probability function of the sample x judged to belong to G_i is 38:

 doi:10.20944/preprints202107.0539.v1

$$P(k|\mathrm{X}) = \frac{q_k f_k(X)}{\sum_{i=1}^{g} q_i f_i(X)} (k = 1, 2, \cdots, g), \tag{4}$$

where q_i is the prior probability of the sample i overall. A series of mathematical transformations of the above function yields the Bayes discriminant function as:

$$F_k(X) = X^T C_k + C_{ok} + \ln q_k = \sum_{j=1}^{m} C_{jk} x_j + C_{ok} + \ln q_k, \tag{5}$$

The posterior probability that sample x belongs to k is the largest when the maximum $F_k(X)$ is taken, and then sample x is determined to belong to the kth overall.

2.3.3. Evaluation of Homogeneity of Silane Coating

In order to reduce the influence of the concrete specimen's own characteristics on the experimental results, the temperature pixel points of the specimen surface before and after spraying silane were clustered and discriminated separately. It is assumed that the clustering values of all pixel points on the concrete surface before spraying silane are set Q, and after spraying silane are set D. The absolute value of the difference between the two is set Z=|Q-D|. If the concrete surface is uniformly coated with silane, the clustering results of the same pixel on the concrete surface before and after the spraying of silane should be the same, i.e. Z=0. Therefore, the uniformity of silane spraying on the concrete surface can be judged qualitatively by counting the difference of the clustering results of each pixel.

Due to the different affiliation of each pixel point obtained from Bayes discriminant calculation, the clustering difference values of each pixel point on the concrete surface before and after spraying the coating are also different. In order to calculate the coating uniformity more accurately, the weight value ω_i of the clustering difference of each pixel point is first calculated using hierarchical analysis. Then the uniformity of the concrete surface coating is calculated according to the magnitude of the weights, and then the uniformity level can be determined. The formula for calculating the non-uniformity of the concrete surface coating can be derived as:

$$U = w_1 \frac{\sum_{j=1}^{n_1} \varepsilon_j}{M} + w_2 \frac{\sum_{j=1}^{n_2} \varepsilon_j}{M} + \ldots + w_i \frac{\sum_{j=1}^{n_i} \varepsilon_j}{M}, \tag{6}$$

where U denotes the unevenness of the concrete surface coating; n_i is the total number of pixel points at Z=*i*; w_1, w_2, ..., w_i are the corresponding weight values; ε_j denotes the affiliation degree corresponding to the jth pixel point; M denotes the total number of pixel points on the concrete surface.

In order to describe the uniformity grade situation of the concrete surface coating, the concrete surface coating uniformity grade can be divided into four grades according to the calculated inhomogeneity U. The specific division grades are shown in Table 1.

Table 1. Classification of concrete surface coating uniformity grade.

Uniformity grade	Very even	More uniform	Uneven	Very uneven
Unevenness U	≤0.1	0.1<U≤0.25	0.25<U≤0.4	>0.4

3. Results

3.1. Infrared Imaging Test Results

Preprints (www.preprints.org) | NOT PEER-REVIEWED | Posted: 23 July 2021 doi:10.20944/preprints202107.0539.v1

A total of 800 seconds of infrared image video streams were acquired for each experiment. Then the IR image processing software ALTAIR was used to export the IR thermal images of the temperature distribution on the surface of the test block. The results of the initial state t=0 and the final state t=800s of the experimental group N1 are shown in Fig. 5 and Fig. 6 as an example.

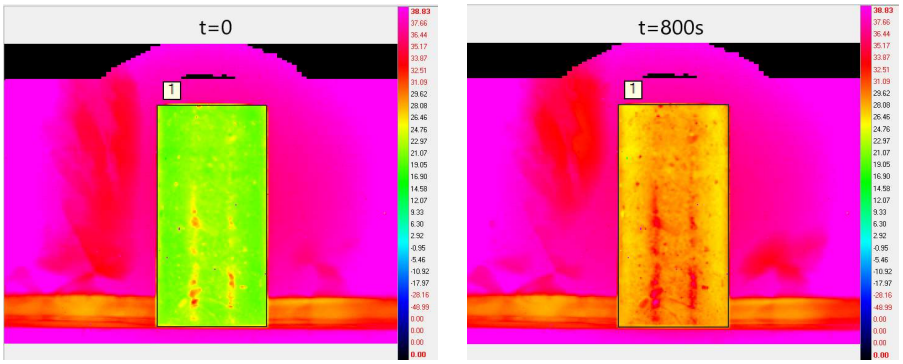

Figure 5. Infrared thermal image of concrete surface before silane spraying.

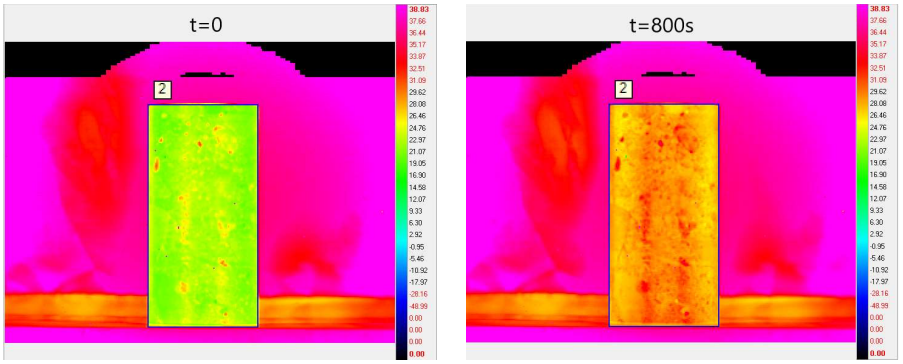

Figure 6. Infrared thermal image of concrete surface after silane spraying.

In order to facilitate the observation and comparison of the silane on the concrete surface temperature change pattern during the heating process, the graph of the average temperature of concrete surface with the number of frames is drawn, as shown in Figure 7.

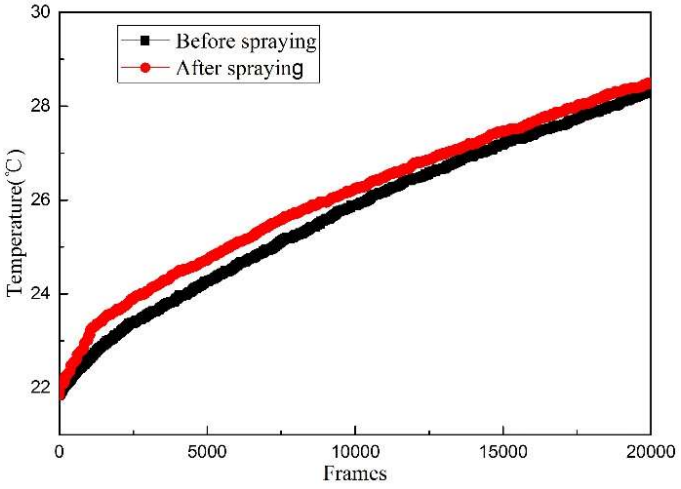

 doi:10.20944/preprints202107.0539.v1

Figure 7. Average temperature-frame variation curve of concrete surface.

By comparing the surface average temperature change law of concrete before and after spraying silane. It can be seen that the average temperature rise rate of concrete structure is accelerated after spraying silane protective coating. This indicates that when silane coating forms a coating structure on the concrete surface, it affects the thermodynamic parameters such as specific heat capacity and thermal conductivity of the concrete structure itself. And when the amount of sprayed silane varies, the degree of its influence will also vary.

3.2. Infrared Image Processing Results

To facilitate the extraction of features from concrete infrared images, different regions of the images need to be labeled. This facilitates the extraction and calculation of the image features. Since the obtained concrete images are binarized, the threshold value can be set to 0. In order to get the effect of the labeling process, the labels are highlighted in MATLAB in different colors to form a pseudo-color image. The image after processing is shown in Figure 8.

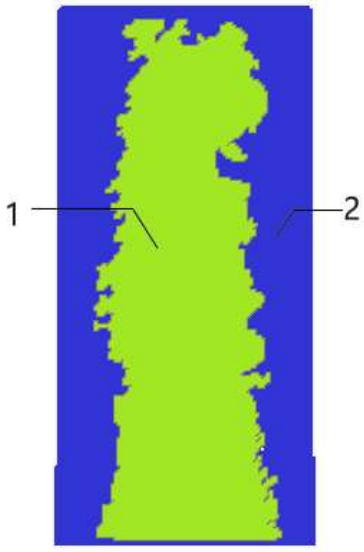

Figure 8. Pseudo-color labeled image.

The area S of each area in the image is used as the basic feature of the infrared image. It is also used as an analytical index to determine the degree of uniformity of the concrete surface coating. In the above figure, 1 and 2 represent different areas of the concrete surface, and the pixel value size of all pixels in area 1 is 1, while the pixel value size of all pixels in area 2 is 2. Therefore, the area size of each area can be calculated by counting the number of pixels in the image with pixel value size 1 and 2, respectively. In turn, the uniformity of the concrete surface coating can be analyzed qualitatively.

3.3. Cluster Analysis Results of Pixel Point Temperature Index

Taking the experimental group N1 as an example, the infrared images of concrete with uncoated silane on the surface are intercepted. The temperature data at different moments corresponding to the corresponding area are derived separately. The region includes a total of 17098 pixel points. The temperature values corresponding to the moments of the 5000th, 10000th, 15000th and 20000th frames are denoted by y1, y2, y3 and y4, respectively, as the indicator variables for each sample point. The final results of the pixel point temperature data statistics are obtained and shown in Table 2.

Preprints (www.preprints.org) | NOT PEER-REVIEWED | Posted: 23 July 2021 doi:10.20944/preprints202107.0539.v1

Table 2. Temperature statistics of each pixel point at different moments.

Sample Pixel Dots	y_1/℃	y_2/℃	y_3/℃	y_4/℃
1	34.01	35.22	35.27	35.29
2	30.76	32.11	32.44	32.64
3	28.47	29.85	30.41	30.85
4	26.72	28.14	28.87	29.48
5	25.46	26.93	27.8	28.51
6	24.6	26.08	27.05	27.81
7	23.75	25.26	26.29	27.15
8	23.01	24.53	25.65	26.57
9	22.87	24.36	25.55	26.45
10	22.43	23.99	25.25	26.16
⋮	⋮	⋮	⋮	⋮
17098	27.97	28.35	29.11	29.56

The clustering analysis for the pixel point temperature data was implemented using the k-means algorithm. The k-values are taken as 2, 3, 4, 5, 6, 7, 8, 9, and 10 in order. And the distance of each pixel point to the cluster center in the cluster it belongs to is calculated by applying SPSS Statistics 19 software. Then the summation was obtained to obtain the magnitude of the error sum of squares corresponding to each different value of k. And the related line graphs were drawn, as shown in Figure 9.

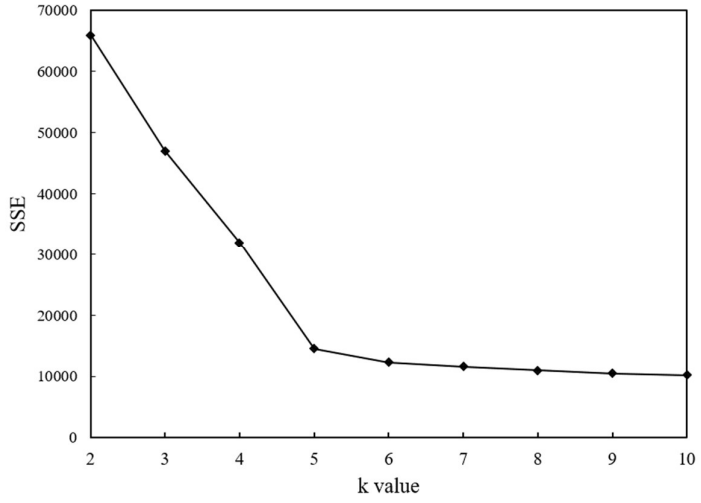

Figure 9. Relationship between SSE and k values.

From the above figure, as the value of the number of clusters k increases, the finer the temperature samples are divided. Therefore, the cohesiveness of the data in each cluster will gradually increase, and the error squared and SSE will naturally become smaller. k=5 is the optimal value for the cluster analysis of pixel point temperature data.

Once the k-values in the algorithm were determined, iterative and classification calculations were performed on the uncoated silane concrete surface temperature data. The four indicator temperature values of the final clustering center and the clustering results of each pixel point are obtained and shown in Table 3 and Table 4.

 doi:10.20944/preprints202107.0539.v1

Table 3. Final clustering center temperature values.

Indicators	Final Clustering Center				
	I	II	III	IV	V
y_1	29.6391	26.5837	24.9286	23.9244	22.7026
y_2	31.1066	28.1504	26.5550	25.5421	24.3250
y_3	32.2659	29.4091	27.9183	26.9281	25.7471
y_4	33.1061	30.3537	28.9340	27.9682	26.8211

Table 4. Clustering results of each pixel point.

Sample Pixel Dots	y_1	y_2	y_3	y_4	Clustering results
1	34.01	35.22	35.27	35.29	I
2	30.76	32.11	32.44	32.64	I
3	28.47	29.85	30.41	30.85	II
4	26.72	28.14	28.87	29.48	II
5	25.46	26.93	27.8	28.51	III
6	24.6	26.08	27.05	27.81	IV
7	23.75	25.26	26.29	27.15	IV
8	23.01	24.53	25.65	26.57	V
9	22.87	24.36	25.55	26.45	V
10	22.43	23.99	25.25	26.16	V
⋮	⋮	⋮	⋮	⋮	⋮
17098	27.97	28.35	29.11	29.56	II

The clustering results show that each pixel point on the concrete surface is clustered into five categories according to the distribution of temperature. Categories I~V indicate the temperature in order from high to low. It can be understood that the concrete surface forms a high temperature zone, a higher temperature zone, a medium temperature zone, a lower temperature zone and a low temperature zone. The number of pixel points in each of these classes is valid. The total number of pixel points in each class was counted, and the results are shown in Figure 10.

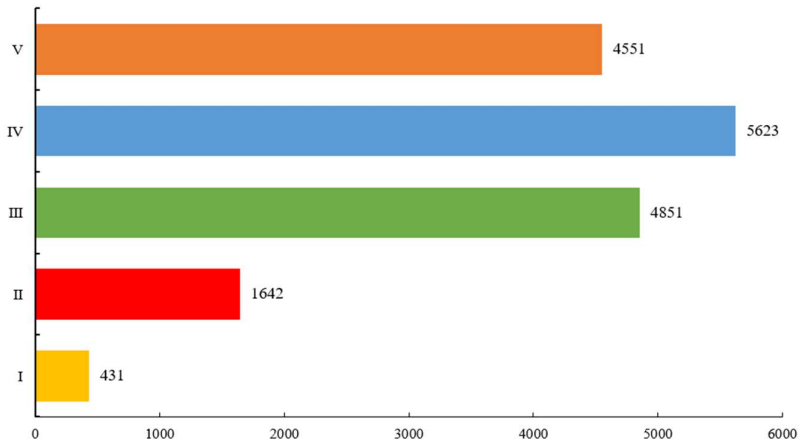

Figure 10. Number of pixel points in each cluster.

 doi:10.20944/preprints202107.0539.v1

As we can be seen from the figure, the largest number of concrete surface pixel points are located in Class IV, accounting for about 32.88% of the entire concrete surface. They are followed by Class III and Class V, accounting for 28.37% and 26.61%, respectively. Class I has the least amount, accounting for only 2.52%. This shows that the medium on the uncoated concrete surface is affected by inhomogeneity, which leads to higher temperatures in some areas than the general area. It shows that this clustering result is consistent with the temperature distribution in the infrared images.

3.4. Pixel Point Affiliation Calculation Results

Based on the clustering analysis results obtained earlier, Bayes discriminant analysis is calculated assuming that the prior probabilities of the points of each overall sample are equal. The formula for calculating the value of the function T for a given pixel point is obtained as follows:

$$\begin{cases} T_1 = -3044.930 + 190.483y_1 - 215.197y_2 - 401.228y_3 + 606.562y_4 \\ T_2 = -2597.086 + 178.761y_1 - 205.079y_2 - 403.184y_3 + 595.286y_4 \\ T_3 = -2390.325 + 178.950y_1 - 216.994y_2 - 393.713y_3 + 589.982y_4 \\ T_4 = -2252.997 + 179.037y_1 - 220.916y_2 - 390.832y_3 + 585.895y_4 \\ T_5 = -2096.145 + 178.281y_1 - 224.798y_2 - 387.047y_3 + 580.708y_4 \end{cases}, \quad (7)$$

The y1, y2, y3, and y4 values of the unknown pixel points are brought into the above equation. The values of T1, T2, T3, T4, and T5 were calculated. And we compared the magnitude of these five values, and took the category corresponding to the maximum value as the Bayesian discriminant result of the pixel point. The values were brought into the posterior probability calculation formula to obtain the posterior probability of each pixel point being discriminated into each category. To determine the cluster affiliation of any pixel point on the concrete surface, the maximum posterior probability value of the pixel point was taken as the affiliation of the pixel point belonging to the corresponding category. Figure 11 represents the two-dimensional distribution of clustering results for each pixel point.

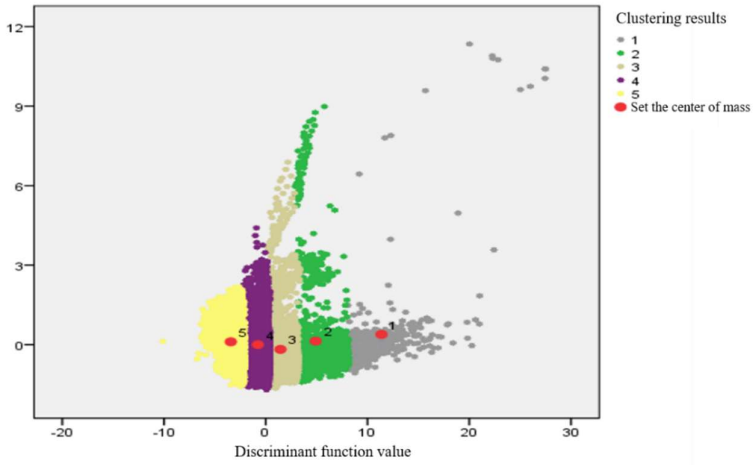

Figure 11. Cluster distribution of pixel points.

In the figure above, each different color represents a different overall class of pixel points clustered into. The individual dots represent the point coordinates of each pixel point projected from the 4-D coordinate system to the 2-D coordinate system. The group

 doi:10.20944/preprints202107.0539.v1

center of mass represents the coordinates of the mean projection of the pixel points in each aggregate to the two-dimensional plane. It can be seen that the distance from the sample points in each aggregate to the respective aggregate center of mass is the smallest. This also further verifies the accuracy of the clustering results obtained from the discriminant analysis. It is not difficult to find that the separation of individual pixel points is larger in the high temperature region and the higher temperature region. This indicates that there are small areas of the concrete surface that are partially defective, leading to discontinuities in the concrete surface temperature and causing sudden temperature rise.

3.5. Coating Uniformity Analysis

The clustering results and the affiliation degree of each pixel point on the concrete surface before and after the coating were calculated for the specimens of the above experimental group N1. The results are shown in Table 5, where the affiliation is the average of the maximum posterior probability of each pixel point.

Table 5. Concrete surface pixel point clustering results before and after silane spraying.

Sample Pixel Dots	Pre-painting results	Results after spraying	Affiliation
1	I	II	1
2	I	I	1
3	II	I	0.99985
4	II	IV	0.99830
5	III	V	0.87697
6	IV	V	0.80302
7	IV	V	0.62214
8	V	V	0.96985
9	V	V	0.98881
10	V	V	0.99867
⋮	⋮	⋮	⋮
17098	II	II	0.99431

The distribution of the variable Z is obtained from the results of the pixel point clustering statistics. The distribution characteristics roughly reflect the uniformity of the surface silane spraying to some extent. The total number of pixels is 6147, 3440, 2179, 1345 when Z=1, 2, 3, 4. Finally, the unevenness of the surface coating of concrete specimens in experimental group N1 can be calculated as U=0.122. The uniformity of the concrete surface coating in this group is evaluated as more uniform. Then the inhomogeneity of the surface coating of concrete specimens in experimental group N2 and experimental group N3 are calculated respectively. The results of their evaluation are obtained and shown in Table 6.

Table 6. Evaluation results of concrete coating uniformity in each experimental group.

Experimental group	N1	N2	N3
Unevenness U	0.122	0.298	0.415
Homogeneity evaluation grade	More uniform	Uneven	Very uneven
Actual painting situation	More uniform	Uneven	Very uneven

It can be seen from table 6 that the evaluation results obtained from the evaluation method of concrete surface coating uniformity based on the combination of cluster analysis and hierarchical analysis are more consistent with the actual spraying situation. Therefore, the method is reasonable and feasible for evaluating the uniformity level of concrete

 doi:10.20944/preprints202107.0539.v1

coating. It can provide some reference value for the uniformity testing and judging in the actual project.

4. Discussion

This study conducts a research on concrete surface coating uniformity detection and its determination and evaluation method. A nondestructive inspection and evaluation method of coating uniformity based on infrared imaging is proposed. We analyzed the images obtained from the non-destructive testing of infrared imaging by using MATLAB software. The characteristics of the infrared images of the concrete surface were obtained, and a method for determining the uniformity of the concrete surface coating by infrared images was proposed. We extracted the temperature distribution data of concrete surface pixel points, and established a new evaluation method of concrete surface coating uniformity based on a combination of cluster analysis and hierarchical analysis. The results show that the determination results obtained by the method are consistent with the actual situation.

We compared the two methods based on MATLAB infrared image analysis processing and based on cluster analysis to determine the uniformity of the concrete surface coating. The results obtained from the image-processing based method are more influenced by environmental factors. The method requires that the concrete structure itself is homogeneous, and also ensures that the concrete surface is heated completely uniformly. Therefore, the accuracy of the determination results obtained by this method is low. For the proposed new method of evaluating the uniformity of surface coating based on cluster analysis, the advantage of this method is that it can eliminate the influence of the characteristics of the concrete specimen itself on the evaluation results. The accuracy of the determination results is also higher.

At present, the application of infrared imaging nondestructive testing technology to detect the uniformity of concrete surface coatings is still in the preliminary stage. The factors affecting the infrared inspection results are many and complex. Coating uniformity testing experiments and processing methods for infrared images are not mature. Therefore, more in-depth research is needed to detect the uniformity of concrete surface coating more scientifically, accurately and quickly. The proposed evaluation method is based on a large sample of temperature data of concrete surface pixel points. When the number of samples is small, the evaluation results obtained by the method may have some errors. Therefore, a more in-depth study of the uniformity evaluation method can be conducted when the number of samples is small. In addition, the evaluation results obtained are a qualitative uniformity rating rather than a quantitatively accurate description of the results. The quantitative study for the uniformity of concrete coatings also needs to be further investigated.

5. Conclusions

In this study, the uniformity of concrete surface coating is taken as the research object. Through the experimental design of infrared imaging inspection of concrete structure, we obtained the infrared thermal images of concrete surface. Based on this, the results obtained from the experiments are processed by applying the statistical methods of MATLAB image processing and cluster analysis, respectively. Finally, we derived a method for determining the uniformity of the concrete surface coating. The main conclusions are as follows:

1. Infrared thermography can determine the uniformity of concrete surface coating by detecting the temperature distribution image on the concrete surface. Therefore, a new nondestructive testing method applicable to concrete surface coating uniformity detection is proposed, infrared imaging nondestructive testing technology.

2. The infrared images acquired in the experiment were analyzed and processed based on MATLAB software. The processing process mainly contains the operations of

image noise removal, edge detection, threshold segmentation and binarization of the images. We derived the final features of the concrete surface images. It can provide a reference for judging the uniformity of concrete surface coating.

3. A new method based on the combination of cluster analysis and hierarchical analysis is proposed to evaluate the study of the uniformity of concrete surface coating. The results show that the evaluation results obtained from the calculation are more consistent with the actual spraying situation. The method can provide some guidance for the application on practical engineering.

In future research, the evaluation of uniformity of temperature data for small samples of concrete surface pixel points can be addressed. As well as the quantitative evaluation of coating uniformity is further investigated.

Author Contributions: Methodology, D.L. and Y.T.; software, F.Q.; validation, W.Z. and Y.J.; formal analysis, W.Z. and F.Q.; data curation, C.G. and F.Q.; writing—original draft preparation, W.Z.; writing—review and editing, D.L. and Y.T.; project administration, D.L. and Y.T.; funding acquisition, D.L. and Y.T. All authors have read and agreed to the published version of the manuscript.

Funding: The research was funded by the Initiation fund for postdoctoral research of Central South University, grant number 228697.

Institutional Review Board Statement: Not applicable.

Informed Consent Statement: Not applicable.

Data Availability Statement: The data that support the findings of this study are available upon request from the authors.

Conflicts of Interest: The authors declare no conflict of interest.

References

1. Zaki, A.; Chai, H. K.; Aggelis, D.G.; Alver, N. Non-destructive evaluation for corrosion monitoring in concrete: a review and capability of acoustic emission technique. *Sensors*. **2015**, *15*, 19069-19101.
2. Hou, B.; Li, X.; Ma, X.; Du, C.; Zhang, D.; Zheng, M.; Ma, F. The cost of corrosion in China. *Npj materials degradation*. **2017**, *1*, 41.
3. Geng, Y.; Li, S.; Hou, D.; Chen, X.; Jin, Z. Effect of SiO_2 sol/silane emulsion in reducing water and chloride ion penetration in concrete. *Coatings*. **2020**, *10*, 682.
4. Zhang, Y.; Li, S.; Zhang, W.; Chen, X.; Hou, D.; Zhao, T.; Li, X. Preparation and mechanism of graphene oxide/isobutyltriethoxy silane composite emulsion and its effects on waterproof performance of concrete. *Construction and building materials*. **2019**, *208*, 343-349.
5. Baltazar, L.; Santana, J.; Lopes, B. Surface skin protection of concrete with silicate-based impregnations: Influence of the substrate roughness and moisture. *Construction and building materials*. **2014**, *70*, 191-200.
6. Park, S.; Kim, Y.Y.; Lee, B.J. Evaluation of concrete durability performance with sodium silicate impregnants. *Advances in materials science and engineering*. **2014**, 945297.
7. Velayutham, T.S.; Majid, W.H.A.; Ahmad, A.B. Synthesis and characterization of polyurethane coatings derived from polyols synthesized with glycerol, phthalic anhydride and oleic acid. *Progress in organic coatings*. **2009**, *66*, 367-371.
8. Petcherdchoo, A. Sensitivity of service life extension and CO_2 emission due to repairs by silane treatment applied on concrete structures under time-dependent chloride attack. *Advances in materials science and engineering*. **2018**, *27*, 93481.
9. Scarfato, P.; DiMaio, L.; Fariello, M.L. Preparation and evaluation of polymer/clay nanocomposite surface treatments for concrete durability enhancement. *Cement & concrete composites*. **2012**, *34*, 297-305.
10. Zanella, C.; Lekka, M.; Rossi, S.; Deflorian, F. Study of the influence of sonication during the electrod eposition of nickel matrix nanocomposite coatings on the protective properties. *Corrosion reviews*, **2011**, *29*, 253-260.
11. Garrido, I.; Laguela, S.; Arias, P. Infrared thermography's application to infrastructure inspections. *Infrastructures*. **2018**, *3*, 353.
12. Vadivambal, R.; Jayas, D.S. Applications of thermal imaging in agriculture and food industry-a review. *Food and bioprocess technology*. **2011**, *4*, 186-199.
13. Qu, Z.; Jiang, P.; Zhang, W. Development and application of infrared thermography non-destructive testing techniques. *Sensors*. **2020**, *20*, 385114.
14. Zhang, H.; Sfarra, S.; Genest, M. A comparative study of enhanced infrared image processing for foreign object detection in lightweight composite honeycomb structures. *International journal of thermophysics*. **2018**, *39*, 140.
15. Kiseleva, Y.V.; Gektin, Y.M., Zaytsev, A.A. Data intercalibration technique for infrared channels of the Elektro-L/MSU-GS imager with the AIRS infrared sounder data. *Izvestiya atmospheric and oceanic physics*. **2016**, *52*, 1181-1190.
16. Bulychev, O.A.; Shleenkov, S.A.; Gusev, O.A. Revealing surface microcracks in metal articles by excitation of high-frequency eddy currents with subsequent infrared-camera imaging. *Russian journal of nondestructive testing*. **2016**, *52*, 457-462.

17. Hardie, R.C.; Hayat, M.M.; Armstrong, E. Scene-based nonuniformity correction with video sequences and registration. *Applied optics*. **2000**, *39*, 1241-1250.
18. Catarius, A.M.; Seal, M.D. Static scene statistical algorithm for nonuniformity correction in focal-plane arrays. *Optical engineering*. **2015**, *54*, 104-111.
19. Rong, S.H.; Zhou, H.X.; Qin, H.L. Guided filter and adaptive learning rate based non-uniformity correction algorithm for infrared focal plane array. *Infrared physics & technology*. **2016**, *76*, 691-697.
20. Moallem, P.; Masoumzadeh, M.; Habibi, M. A novel adaptive Gaussian restoration filter for reducing periodic noises in digital image. *Signal image & video processing*. **2015**, *9*, 1-13.
21. Forbus, K.D. Qualitative process theory. *Artificial intelligence*. **1984**, *24*, 85-168.
22. Sulaiman, S.N.; Isa, A.M. Adaptive fuzzy-K-means clustering algorithm for image segmentation. *IEEE Transactions on Consumer Electronics*. **2010**, *56*, 2661-2668.
23. Diday, E.; Simon, J.C. Clustering analysis. *Digital pattern recognition*. **1980**,*10*, 47-94.
24. Steinley, D. Local optima in k-means clustering: what you don't know may hurt you. *Psychological methods*, **2003**, *8*, 294-304.
25. MacQueen, J.B. Some methods for classification and analysis of multivariate observations. Proceedings of the 5th berkeley symposium on mathematical statistics and probability. Berkeley, Calif, USA. University of California Press, 1967, *1*, 281–297.
26. Evans, S.; Lloyd, J.; Stoddard, G.; Nekeber, J.; Samone, M. Risk factors for adverse drug events. *The annals of pharmacotherapy*. **2005**, *39*, 1161-1168.
27. David, W.B.; Elizabeth, B.; Miller, D.J.; Cullen, L.B.; Lawrence, W.; Nan, L.; Laura, A.P.; Stephen, D.S.; Bobbie, J.S.; Martha, V.V.; Lucian, L.L. Patient risk factors for adverse drug events in hospitalized Işık M., Data with partitioned clustering methods mining practices. Master Thesis, Institute of Science, Istanbul, 2006, 76p.
28. Li, S.; Jin, W.; Li, L.; Liu, M.; Yang, J. Fusion algorithm based on grayscale-gradient estimation for infrared images with multiple integration times. *Infrared physics & technology*. **2020**, *105*, 103179.
29. Khaw, H.Y.; Soon, F.C.; Chuah, J.H.; Chow, C. High-density impulse noise detection and removal using deep convolutional neural network with particle swarm optimisation. *Iet image processing*. **2019**,*13*, 365-374.
30. Suzuki, K.; Oho, E. Feature evaluation of complex hysteresis smoothing and its practical applications to noisy sem images. *Scanning*. **2013**, *35*, 292-301.
31. Sun, C.; Tang, C.; Zhu, X.; Li, X.; Wang, L.. An efficient method for salt-and-pepper noise removal based on shearlet transform and noise detection. *Aeu-international journal of electronics and communications*. **2015**, *69*, 93-102.
32. Xu, J.; Ye, L.; Luo, W. Color edge detection using multiscale quaternion convolution. *International journal of imaging systems and technology*. **2010**, *20*, 354-358.
33. Xu, C.; Han, W.; Wang, D.; Huang, D. Salient region detection with multi-feature fusion and edge constraint. *Ieice transactions on information and systems*, **2020**, *103*, 4.
34. Said, K.A.M.; Jambek, A.B. A study on image processing using mathematical morphological *International conference on electronic design*. **2016**, *1*, 507-512.
35. Zhang, H.; Yu, H.; Li, Y.; Hu, B. Improved K-means Algorithm Based on the Clustering Reliability Analysis. *ACSR-advances in comptuer science research*. **2015**, *13*, 2516-2523.
36. Lakshmi, R.; Baskar, S. DIC-DOC-K-means: dissimilarity-based initial centroid selection for DOCument clustering using K-means for improving the effectiveness of text document clustering. *Journal of information science*. **2019**, *45*, 818-832.
37. Subedi, S.; McNicholas, P.D. Variational Bayes approximations for clustering via mixtures of normal inverse Gaussian distributions. *Advances in data analysis and classification*. **2014**, *8*, 167-193.
38. Zhang, J.; Wang, S.; Chen, L. Multiple Bayesian discriminant functions for high-dimensional massive data classification. *Data mining & knowledge discovery.* **2017**, *31*, 1-37.